Published in final edited form as:
Hepatology. 2008 April ; 47(4): 1191–1199.

Loss of the Glycine *N*-Methyltransferase Gene Leads to Steatosis and Hepatocellular Carcinoma in Mice

M. Luz Martínez-Chantar[1,*], **Mercedes Vázquez-Chantada**[1,*], **Usue Ariz**[1], **Nuria Martínez**[1], **Marta Varela**[1], **Zigmund Luka**[2], **Antonieta Capdevila**[2], **Juan Rodríguez**[1], **Ana M. Aransay**[1], **Rune Matthiesen**[1], **Heping Yang**[3], **Diego F. Calvisi**[4], **Manel Esteller**[5], **Mario Fraga**[5], **Shelly C. Lu**[3], **Conrad Wagner**[2,6], and **José M. Mato**[1]

1*CIC bioGUNE, CIBERehd, Technology Park of Bizkaia, Bizkaia, Spain*

2*Department of Biochemistry, Vanderbilt University, Nashville, TN*

3*Division of Gastrointestinal and Liver Diseases, Keck School of Medicine, University Southern California, Los Angeles, CA*

4*Division of Experimental Pathology and Oncology, University of Sassary, Sassary, Italy*

5*Centro Nacional de Investigaciones Oncológicas, Madrid, Spain*

6*Tennessee Valley Department of Medical Affairs Medical Center, Nashville, TN*

Abstract

Glycine *N*-methyltransferase (GNMT) is the main enzyme responsible for catabolism of excess hepatic S-adenosylmethionine (SAMe). GNMT is absent in hepatocellular carcinoma (HCC), messenger RNA (mRNA) levels are significantly lower in livers of patients at risk of developing HCC, and GNMT has been proposed to be a tumor-susceptibility gene for liver cancer. The identification of several children with liver disease as having mutations of the *GNMT* gene further suggests that this enzyme plays an important role in liver function. In the current study we studied development of liver pathologies including HCC in GNMT-knockout (GNMT-KO) mice. GNMT-KO mice have elevated serum aminotransferase, methionine, and SAMe levels and develop liver steatosis, fibrosis, and HCC. We found that activation of the Ras and Janus kinase (JAK)/signal transducer and activator of transcription (STAT) pathways was increased in liver tumors from GNMT-KO mice coincidently with the suppression of the Ras inhibitors Ras-association domain family/tumor suppressor (RASSF) 1 and 4 and the JAK/STAT inhibitors suppressor of cytokine signaling (SOCS) 1-3 and cytokine-inducible SH2-protein. Finally, we found that methylation of *RASSF1* and *SOCS2* promoters and the binding of trimethylated lysine 27 in histone 3 to these 2 genes was increased in HCC from GNMT-KO mice.

Conclusion—These data demonstrate that loss of GNMT induces aberrant methylation of DNA and histones, resulting in epigenetic modulation of critical carcinogenic pathways in mice.

The first steps in mammalian methionine metabolism are conversion to S-adenosylmethionine (SAMe) and transfer of the methyl group of SAMe to a large variety of substrates (including DNA, RNA, histones, and small molecules such as glycine, guanidinoacetate, and phosphatidylethanolamine) with the formation of S-adenosylhomocysteine (SAH), an inhibitor of many SAMe-dependent methyltransferases.[1] Although there are a large number of SAMe-

Address reprint requests to: José M Mato, CIC bioGUNE, Technology Park of Bizkaia, 48160 Derio, Bizkaia, Spain. E-mail: director@cicbiogune.es; fax: (34) 944-061301.
*These authors contributed equally to this article.

Published online in Wiley InterScience (www.interscience.wiley.com).

Potential conflict of interest: Nothing to report.

dependent methyltransferases,[2] methylation of glycine by glycine *N*-methyltransferase (GNMT) to form sarcosine (*N*-methylglycine) is one of the reactions that contribute most to total transmethylation flux.[3] The importance of GNMT is to remove excess SAMe and maintain a constant hepatic SAMe/SAH ratio to avoid aberrant methylation.[2] Consistent with this function, the activation of GNMT in rats by the administration of retinoic acid causes a reduction in plasma methionine and homocysteine levels, as well as in liver DNA methylation.[4,5] In GNMT-knockout (GNMT-KO) mice, liver SAMe content is elevated 35-fold, and the SAMe/SAH ratio increases about 100-fold,[6] and individuals with GNMT mutations, which leads to inactive forms of the enzyme, have elevated plasma levels of methionine and SAMe but a normal concentration of homocysteine.[7,8]

GNMT is expressed in the liver, pancreas, and prostate[9] and is absent in hepatocellular carcinoma (HCC)[10] and down-regulated in the livers of patients at risk of developing HCC, such as in those with hepatitis C virus–and alcohol-induced cirrhosis.[11] Moreover, a loss of heterozygosity of *GNMT* has been reported in about 40% of HCC patients, and *GNMT* has been proposed to be a tumor-susceptibility gene for liver cancer.[12,13] Identification of several children with mutations of GNMT as having mild to moderate liver disease with elevated serum aminotransferases[7,8] further suggests that a defect in this enzyme leads to liver disease.

To define the role of GNMT in the liver, we examined hepatic function in GNMT-KO mice. The GNMT-deficient mice recapitulated the situation observed in individuals with mutations in GNMT[7,8] and showed elevated serum aminotransferases, methionine, and SAMe levels. Moreover, the GNMT-KO mice developed steatosis, fibrosis, and HCC. Finally, we analyzed the activation of the Ras and Janus kinase (JAK)/signal transducer and activator of transcription (STAT) pathways in GNMT-KO mice, as well as the methylation of DNA and H3K27, which may result in epigenetic modulation of critical carcinogenic pathways.

Materials and Methods

Animal Experiments

The generation of GNMT-KO mice has been described.[6] All animal experimentation was conducted in accordance with the Spanish Guide for the Care and Use of Laboratory Animals, and protocols were approved by the CIC bioGUNE Ethical Review Committee. Three-month-old and 8-month-old male homozygous GNMT-KO and their wild-type (WT) littermates were killed for histological examination of their livers. In addition, liver specimens were snap-frozen for subsequent analysis. At the time of death, serum samples were collected for determination of alanine aminotransferase (ALT) and aspartate aminotransferase (AST) levels or deproteinized with acetonitrile for methionine and SAMe analysis.

Measurement of Methionine and SAMe

Serum levels of methionine and SAMe were determined by liquid chromatography/mass spectrometry (LC/MS) using a Waters Acquity ultraperformance liquid chromatography (UPLC) system equipped with a column oven, and a Waters Acquity UPLC BEH C_{18} column (2.1 × 100 mm, 1.7 μm). A 3-μL aliquot of sample was injected into the UPLC column, which was maintained at 50°C and eluted at 600 μL/min. The mobile phase consisted of water with 0.05% formic acid (solvent A) and acetonitrile with 0.05% formic acid (solvent B). Separation was carried out starting with 1% B for 1 minute, followed by a linear gradient from 1% to 95% B for 10 minutes and staying at 95% B for 6 minutes. The UPLC system was coupled to a Waters Micromass LCT Premier Mass Spectrometer equipped with a Lockspray ionization source operating in electrospray positive ion mode (W mode, resolution 10,000 full width at half maximum). Full-scan time-of-flight MS spectra were acquired between *m/z* (mass-to-charge ratio) 80 and 1,000 using the dynamic range enhancement mode, with a total scan time

of 0.4 seconds. Leucine enkephalin was used as a reference compound for accurate mass measurements. The reference was infused into the Lockspray reference channel, and the masses of the analyte channel were automatically mass-corrected by the software. A set of samples, prepared from all standard compounds, was acquired over the concentration range of 10 pg/μL to 50 ng/μL in order to test the linearity of the system. After analyzing all concentration levels, calibration curves were generatedμL and chromatogram traces of the protonated species of the standards were extracted with a mass window of 0.05 Da. Serum levels of methionine and SAMe were automatically calculated from the calibration curves.

Histology and Immunohistochemistry

Sections from formalin-fixed liver tissue were stained with hematoxylin and eosin or with Sirius red for collagen visualization. The proliferation marker Ki67 was evaluated by immunostaining using mouse monoclonal anti-Ki67 primary antibody.

Quantitative Real-Time PCR

Total liver RNA was isolated by the guanidinium thiocyanate method. RNA concentration was determined spectrophotometrically before use, and integrity was checked by electrophoresis with subsequent ethidium bromide staining. The RNA was purified with an RNeasy Mini kit (Qiagen, Chatsworth, CA) including DNase treatment. Two micrograms of total RNA were then retrotranscribed with the M-MLV retrotranscriptase (Promega, Madison, WI) in the presence of an oligo dT. We performed quantitative real-time polymerase chain reaction (PCR) in a Bio-Rad iCycler thermalcycler (Bio-Rad Laboratories, Hercules, CA). All samples were run in triplicate. Five microliters of a 1:20 dilution of cDNA was used in each PCR reaction in a total reaction volume of 30 μL using iQ SYBR Green Super Mix (Bio-Rad). Primers were designed with Primer Express Software (Applied Biosystems, Foster City, CA) to determine the expression of Ras-association domain family/tumor suppressor (RASSF)–1, RASSF4, cytokine-inducible SH2-protein (CIS), SOCS1, SOCS2, SOCS3, ADFP, UCP2, CYP4A10, CYP4A14, TIMP-1, and iNOS and synthesized by Invitrogen. After checking the specificity of the PCR products with the melting curve, *Ct* values were extrapolated to a standard curve performed simultaneously with the samplesμL and data were then normalized to GAPDH expression. The complete list of primer sequences used and the PCR conditions are available on request.

Western Blotting

Samples were separated by SDS-PAGE and analyzed by immunoblotting using commercial antibodies. Blots were developed with secondary antirabbit or antimouse antibodies conjugated to horseradish peroxidase (Invitrogen, Carlsbad, CA) and the luminal-chemiluminescence reagent (ECL; Amersham Biosciences, Upsala, Sweden). The processed blots were exposed to X-ray film, and the autoradiograms were analyzed.

Ras Activity

Liver tissue samples were homogenized in lysis buffer [125 mM HEPES (pH 7.5), 750 mM NaCl, 5% Igepal CA-630, 50 mM $MgCl_2$, 5 mM EDTA, and 10% glycerol] containing Complete Protease Inhibitor Cocktail (Roche Molecular Biochemicals) and sonicated. Protein concentrations were determined with a Bio-Rad Protein Assay Kit using bovine serum albumin as a standard. Aliquots of 800 μg of tissue lysates were immunoprecipitated with 5 μg of mouse monoclonal anti–pan Ras antibody (sc-32; Santa Cruz Biotechnology, Santa Cruz, CA). Immunoprecipitated proteins were denatured by boiling in Tris-Glycine SDS Sample Buffer (Novex-Invitrogen, Carlsbad, CA), separated by SDS-PAGE, and then transferred onto nitrocellulose membranes (Novex-Invitrogen) by electroblotting. The membranes were blocked in 5% nonfat dry milk in Tris-buffered saline containing 0.1% Tween 20 for 1 hour

and probed with the rabbit polyclonal anti-RAF-1 antibody (sc-133, Santa Cruz Biotechnology) in a 1:2,000 dilution. Immunoprecipitated proteins were revealed via enhanced chemiluminescence (Amersham), and the bands were quantified in arbitrary units by ImageMaster Total Lab V1.11 software and normalized to actin levels (as detected with the rabbit polyclonal antiactin antibody sc-10731; Santa Cruz Biotechnology).

Global DNA Methylation and DNA Methyltransferase Activity

5-Methylcytosine (5mC) genomic content was determined by high-performance capillary electrophoresis, as described.[14] Briefly, genomic DNA samples were boiled, treated with nuclease P1 (Sigma) for 16 hours at 37°C and with alkaline phosphatase (Sigma) for an additional 2 hours at 37°C. After hydrolysis, total cytosine and 5mC content were measured by capillary electrophoresis using a P/ACE MDQ system (Beckman-Coulter). All samples were analyzed in triplicate. Relative 5mC content was expressed as a percentage of total cytosine content (methylated and nonmethylated). DNA methyltransferase activity was measured using an EpiQuick DNA methyltransferase Activity kit.

Sequence-Specific DNA Methylation

The CpG DNA methylation status of a subtelomeric DNA region at chromosome 1 and of the promoters of *RASSF1* and *SOCS2* was established by PCR analysis after bisulfite modification. Bisulfite genomic sequencing of multiple clones was then carried out as described elsewhere.[15] The primers used were: 5′-AAAAGATGGTGAGTGTAGGTGT-3′ (sense) and 5′-TCACAATATCCTCCTCTTCTTC-3′ (antisense) for chromosome 1; 5′-CGAACGTGGTGAGCGCGG-3′(sense) and 5′-CGCCCCTCGACGTCTTCACCCCCTCAC-3′ (antisense) for *RASSF1*; and 5′-TGTCTCCCTCCTCACCCCTCTACTCCGG-3′ (sense) and 5′-ACGCGAGGTCCACTGGCCCCAGC-3′ (antisense) for *SOCS2*.

Promoter Methylation

*Msp*I and *Hpa*II restriction endonucleases were used as described with modifications.[16] *Msp*I and *Hpa*II can distinguish between unmethylated and methylated cytosine in the nucleotide sequence 5′-CCGG. *Msp*I is insensitive to the methylation status, whereas *Hpa*II will digest only if the internal cytosine is unmethylated.[26] DNA samples (30 μg each) were first digested with *Stu*I and *Bbv*I for *RASSF1* or *Bspm*II and *Tthlll*I for *SOCS2* at 37°C for 4 hours. This was followed by overnight digestion with *Hpa*II or *Msp*I at 37°C. The digested DNA was separated on 1% agarose, transferred onto nylon filters by 20× standard sodium citrate (SSC), and cross-linked in an ultraviolet cross-linker (FS-UVXL-1000, Fisher Biotech). The filters were prehybridized at 42°C in Rapid-Hybridization Buffer (Ambion, Austin, TX) for 2 hours and hybridized with the [^{32}P]dCTP-labeled *RASSF1* probe (corresponding to −313 to −780 base pairs upstream of the mouse *RASSF1* translational start site, GenBank accession number NM_019713) or the *SOCS2* probe (corresponding to −205 to −511 base pairs upstream of the mouse *SOCS2* translational start site, GenBank accession number NM_007706) for 8 hours at 42°C in the same buffer. The blots were washed at 42°C for 20 minutes in 2× SSC containing 0.1% SDS twice and at 42°C for 30 minutes in 0.1×SSC containing 0.1% SDS. Autoradiography was performed by exposure to Kodak BioMax MR film at −80°C.

Analysis of Trimethylated Lysine 27 in Histone 3

Chromatin immunoprecipitation assay was carried out as described[15] using antibodies against trimethylated lysine 27 in histone 3 (H3K27me3; Abcam). Chromatin was sheared to an average length of 0.25 ± 1 kb, and PCR amplification was performed in 96-well optical plates in a volume of 20 μL. We used 15 ng of immunoprecipitated DNA, 5 pmol of each primer, and 10 μL of 2× SYBRGreen PCR master Mix (Applied Biosystems). All measurements were

carried out in triplicate, and amounts were calculated extrapolating from a standard curve. The primers and conditions for each promoter are available on request.

Statistical Analysis

The Student *t* test was used to evaluate statistical significance. *P* values < 0.05 were considered statistically significant.

Results

Deletion of GNMT Gene Induces Steatosis, Fibrosis, and Hepatocellular Carcinoma

To define the metabolic role of GNMT in the liver, we examined hepatic function in GNMT-KO and WT male mice. The GNMT-deficient mice recapitulated the situation observed in children with mutations in GNMT[8,9] and showed elevated serum aminotransferases, methionine and SAMe at both 3 and 8 months of age (Table 1). Histological examination of the livers of 3-month-old mutant mice showed steatosis and fibrosis, which were more prominent in the livers of 8-month-old mice (Fig. 1A). No significant signs of inflammation were observed at either 3 or 8 months of age. At 8 months, all GNMT-KO mice (n = 10) also developed multifocal HCC, as determined by staining with hematoxylin and eosin and with the cellular proliferation marker Ki67 (Fig. 1). The number of liver tumors varied from 2 to 9, with an average of 4 tumors per mouse. No evidence of focal hyperplasic lesions was observed in GNMT-KO livers at 3 or 5 months of age. Histological examination of prostate, pancreas, and kidney did not reveal signs of tumor formation in 8-month-old GNMT-KO mice.

Activation of Ras and JAK/STAT Pathways in HCC from GNMT-Deficient Mice

HCC in humans is characterized by the persistent activation of the Ras/mitogen-activated/extracellular-regulated kinase (MEK)/extracellular signal-regulated kinase (ERK) and JAK/STAT signaling pathways via suppression of Ras and JAK/STAT inhibitors such as RASSF1, CIS, and SOCS1, SOCS2, and SOCS3.[17-21] Accordingly, we observed that the expression of Ras inhibitors RASSF1 and RASSF4 and of JAK/STAT inhibitors SOCS1, SOCS2, SOCS3, and CIS was reduced in liver tumors from 8-month-old GNMT-KO male mice (Table 2). Concomitant with the loss of Ras inhibitors, Ras and downstream effectors of Ras involved in proliferation and survival, including pRaf, pMEK1/2, and pERK1/2, were activated in liver tumors from GNMT-deficient mice (Fig. 2A). Ras activity, assessed by immunoprecipitation with anti–pan Ras antibody and probed with anti-RAF-1 antibody, was also markedly increased in liver tumors from 8-month-old GNMT-mutant mice (Fig. 2B). Similarly, suppression of JAK/ STAT inhibitors in liver tumors from GNMT-KO mice was associated with the activation of the JAK/STAT signaling pathway, including proliferation proteins cyclin D1 and cyclin D2 and the antiapoptotic protein Bcl-xL (Fig. 2C). In these experiments we analyzed the liver containing tumors but not the surrounding liver. We chose to compare tumors to age-matched WT controls because the surrounding liver tissue may also be abnormal, as suggested by the finding that the expression of Ras and JAK/STAT inhibitors was already reduced in liver samples from 3-month-old GNMT-KO male mice (Table 2) and by the observation that Ras activity was also markedly increased in 3-month-old GNMT-KO mice liver (Fig. 2B).

Increased Promoter Methylation and Binding to H3K27me3 of RASSF1 and SOCS2 in HCC from GNMT-KO Mice

Because the importance of GNMT is to remove excess SAMe and maintain a constant SAMe/SAH ratio to avoid aberrant methylation reactions,[2] we hypothesized that the loss of GNMT may lead to abnormal DNA and histone methylation of specific and critical carcinogenic pathways. First, we assessed global DNA methylation and the methylation of a subtelomeric DNA region of chromosome 1 and found both to be hypermethylated in 8-month-old GNMT-

KO male mice (Fig. 3A,B). Given that the inhibitors of the Ras and JAK/STAT signaling pathways are frequently inactivated by promoter methylation,[17,19-21] we then examined the methylation of RASSF1 and *SOCS2* promoters. Methylation-sensitive Southern blot analysis showed hypermethylation of these 2 promoters in liver tumors from 8-month-old GNMT-mutant mice (Fig. 3D,E). Because H3K27me3 is an epigenetic marker highly associated with genomic silencing,[22] we also examined the trimethylation of H3K27 bound to *RASSF1* and *SOCS2* promoters. As shown in Fig. 3F,G, the level of H3K27me3 bound to *RASSF1* and *SOCS2* increased about 2-fold in liver tumors from GNMT-KO mice as compared with WT animals.

Finally, we analyzed whether epigenetic pathways observed in the liver tumors were activated in 3-month-old mice before histological evidence of tumor development. As shown in Fig. 3, global DNA methylation, CpG DNA methylation of a subtelomeric DNA of chromosome 1, promoter methylation of *RASSF1* and *SOCS2* promoters, and trimethylation of H3K27 bound to *RASSF1* and *SOCS2* promoters were all significantly increased in liver samples from 3-month-old GNMT-deficient mice as compared to WT liver samples. To determine the CpG DNA methylation status of *RASSF1* and *SOCS2* promoters in liver samples from 3-month-old mice, we employed bisulfite genomic sequencing because the less sensitive technique used with livers from 8-month-old mice, based on the use of *Msp*I and *Hpa*II restriction endonucleases, did not reveal differences between GNMT-KO and WT livers from 3-month-old mice.

Liver DNA methyltransferase activity was similar in GNMT-deficient mice and WT animals at 3 month of age, whereas it was significantly increased (1.6 ± 0.2 fold, $P < 0.05$, $n = 5$) in the HCC nodules of 8-month-old GNMT-KO mice. These results suggest that epigenetic changes in GNMT-KO mice are most probably at least initially a result of the accumulation of SAMe and the increased SAMe/SAH ratio in the livers of these animals.

Discussion

GNMT is the most abundant methyltransferase in mammalian liver.[9] GNMT catalyzes the conversion of glycine into sarcosine, which is then oxidized to regenerate glycine. The function of this futile cycle is to catabolize excess liver SAMe to maintain a constant SAMe/SAH ratio in order to avoid aberrant methylation reactions.[1-3] Accordingly, the loss of GNMT in mice leads to the accumulation of hepatic SAMe and to a marked increase in the hepatic SAMe/SAH ratio without affecting SAH levels,[6] and the activation of GNMT in rats by the administration of retinoic acid causes a reduction in global liver DNA methylation.[4]

In the present study, we showed that GNMT-deficient mice recapitulate the situation observed in individuals with mutations of the *GNMT* gene[7,8] and have elevated serum aminotransferases, methionine, and SAMe. Moreover, in this study we showed that GNMT-deficient mice spontaneously develop steatosis, fibrosis, and HCC. These results support the concept that GNMT is a tumor-susceptibility gene for liver cancer[12] and further suggest that reduced GNMT activity may be an early event in the development of HCC. Recently, the phenotype of a GNMT-KO mouse model that differs from ours was published.[18] Consistent with the present results and with our previous observations,[6] this other GNMT-KO mouse model has hypermethioninemia and elevated levels of both serum ALT and hepatic SAMe.[18] However, these knockout mice did not develop steatosis or HCC, but about 60% of the animals had increased glycogen storage in the livers, as determined by staining with PAS.[18] In the article by Liu et al.,[18] no evidence about the molecular mechanism by which an increase in hepatic SAMe content induces glycogen storage is provided. In our GNMT-KO mouse model, hepatic PAS staining showed no differences between WT and knockout mice in glycogen staining (not shown). We believe that high SAMe levels can produce epigenetic

changes that may differ depending on the genetic background and other factors such as nutritional factors, and it is possible this is why the phenotypes differ. Nevertheless, our finding of liver cancer development in GNMT-KO mice is consistent with the reported role of GNMT as a tumor suppressor in human hepatocellular carcinoma.

Previous studies have demonstrated that the Ras and JAK/STAT pathways are universally activated in human HCC and that the activation of these pathways may be essential for HCC development.[17] We have observed that, as in human HCC, the Ras and JAK/STAT pathways are activated in liver tumors from GNMT-deficient mice and that, as also found in human HCC, [17] activation of these signaling pathways coincided with suppression of the Ras and JAK/STAT inhibitors *RASSF1, RASSF4, SOCS1, SOCS2, SOCS3*, and *CIS*. These inhibitors of the Ras and JAK/STAT signaling pathways, which are frequently inactivated by promoter methylation, have been involved in carcinogenesis.[17,19-22,24,25] Epigenetic inactivation of *RASSF1* is one of the most common molecular changes in cancer; and a direct correlation between promoter methylation and loss of *RASSF1* expression has been shown in many tumor cell lines including hepatoma.[17,24] Similarly, the frequency of promoter hypermethylation of *SOCS2* has been found to occur in more than 80% of both human HCC and hepatoma cell lines and to correlate with the loss of SOCS2 expression.[17] Consistent with these findings, our data demonstrate that the methylation of *RASSF1* and *SOCS2* promoters is increased in liver tumors from GNMT-knockout mice. Promoter hypermethylation in cancer cells is known to be associated with a variety of alterations in histone modification, including increased H3K27 methylation, which is linked to gene repression.[26] Our observation that the level of H3K27me3 bound to *RASSF1* and *SOCS2* was increased in liver tumors of GNMT-KO mice agrees with this concept. Moreover, our results also indicate that the epigenetic pathways observed in the liver tumors were activated in 3-month-old mice, well in advance of any histological evidence of tumor formation, strongly suggesting a pathogenic relationship between methylation changes and hepatocarcinogenesis.

We have previously demonstrated[27,28] that in mice deficient in hepatic SAMe synthesis (methionine adenosyl-transferase 1A knockout mice), SAMe levels in the liver and the SAMe/SAH ratio are reduced and that these animals spontaneously develop steatohepatitis and HCC. Mice deficient in other key enzymes of methionine and folate metabolism, such as cystathionine β synthase and methylenetetrahydrofolate reductase, also have altered levels of hepatic SAMe and a reduced SAMe/SAH ratio and spontaneously develop fatty liver disease.[29,30] These findings, together with the present observations using mice deficient in GNMT, suggest that either too much or too little hepatic SAMe in concert with abnormal SAMe/SAH ratios may result in aberrant methylation of DNA and histones, resulting in epigenetic modulation of critical metabolic and carcinogenic pathways in mice, which emphasizes the crucial role of methionine and folate metabolism in maintaining normal liver function.[1]

Acknowledgements

The authors thank B. Rodríguez for technical assistance, F. Muruzabal for help with the histological preparations, G. Kanel for help with the interpretation of the histology, and OWL Genomics for methionine and SAMe analysis.

Supported by NIH grants AA12677, AA13847, and AT-1576 (to S.C.L. and J.M.M.); DK15289 (to C.W.), PN I+D SAF 2005-00855, HEPADIP-EULSHM-CT-205, and ETORTEK 2005 (to J.M.M. and M.L.M.-C.); Program Ramón y Cajal (to M.L.M.-C.); and Fundación “La Caixa” (to M.L.M.-C., R.M., and A.M.A.).

References

1. Mato JM, Lu SC. Role of S-adenosyl-L-methionine in liver health and injury. Hepatology 2007;45:1306–1312. [PubMed: 17464973]

2. Clarke, S.; Banfield, K. S-Adenosylmethionine-dependent methyltransferase. In: Carmel, R.; Jacobsen, DW., editors. Homocysteine in Health and Disease. Cambridge, UK: Cambridge University Press; 2001. p. 63-78.
3. Mudd SH, Brosnan JT, Brosnan ME, Jacobs RL, Stabler SP, Allen RH, et al. Methyl balance and transmethylation fluxes in humans. Am J Clin Nutr 2007;85:19–25. [PubMed: 17209172]
4. Rowling MJ, McMullen MH, Schalinske KL. Vitamin A and its derivatives induce hepatic glycine N-methyltransferase and hypomethylation of DNA in rats. J Nutr 2002;132:365–369. [PubMed: 11880556]
5. Ozias M, Schalinske KL. All-trans-retinoic acid rapidly induces glycine N-methyltransferase in a dose-dependent manner and reduces circulating methionine and homocysteine levels in rats. J Nutr 2003;133:4090–3094. [PubMed: 14652353]
6. Luka Z, Capdevila A, Mato JM, Wagner C. A glycine N-methyltransferase knockout mouse model for humans with deficiency of this enzyme. Transgenic Res 2006;15:393–397. [PubMed: 16779654]
7. Mudd SH, Cerone R, Schiaffino MC, Fantasia AR, Minniti GU, Caruso U, et al. Glycine N-methyltransferase deficiency: a novel inborn error causing persistent isolated hypermethioninaemia. J Inherit Metab Dis 2001;24:448–464. [PubMed: 11596649]
8. Augoustides-Savvopoulou P, Luka Z, Karyda S, Stabler SP, Allen RH, Patsiaoura K, et al. Glycine N-methyltransferase deficiency: a new patient with a novel mutation. J Inherit Metab Dis 2003;26:745–749. [PubMed: 14739680]
9. Ogawa H, Fujikoa M. Purification and properties of glycine N-methyltransferase from rat liver. J Biol Chem 1982;257:3447–3452. [PubMed: 6801046]
10. Chen YM, Shiu JY, Tzeng SJ, Shih LS, Chen YL, Lui WY, Chen PH. Characterization of glycine-N-methyltransferase-gene expression in human hepatocellular carcinoma. Int J Cancer 1998;75:787–793. [PubMed: 9495250]
11. Avila MA, Berasain C, Torres L, Martin-Duce A, Corrales FJ, Yang H, et al. Reduced mRNA abundance of the main enzymes involved in methionine metabolism in human liver cirrhosis and hepatocellular carcinoma. J Hepatol 2000;33:907–914. [PubMed: 11131452]
12. Tseng TL, Shih YP, Huang YC, Wang CW, Chen PH, Chang JG, et al. Genotypic and phenotypic characterization of a putative tumor susceptibility gene, GNMT, in liver cancer. Cancer Res 2003;63:647–654. [PubMed: 12566309]
13. Chen SY, Lin JR, Darbba R, Lin P, Liu TY, Chen YM. Glycine N-methyltransferase tumor susceptibility gene in the benzo(a)pyrene-detoxification pathway. Cancer Res 2004;64:3617–3623. [PubMed: 15150120]
14. Fraga MF, Ballester E, Villar-Garea A, Boix-Chornet M, Espada J, Schotta G, et al. High-performance capillary electrophoretic method for the quantification of 5-methyl 2′-deoxycytidine in genomic DNA: application to plant, animal and human cancer tissues. Electrophoresis 2002;23:1677–1681. [PubMed: 12179987]
15. Fraga MF, Ballester E, Villar-Garea A, Boix-Chornet M, Espada J, Schotta G, et al. Loss of acetylation at Lys16 and trimethylation at Lys20 of histone H4 is a common hallmark of human cancer. Nat Genet 2005;37:391–400. [PubMed: 15765097]
16. Garcea R, Daino L, Pascales R, Simile MM, Puddu M, Ruggiu ME, et al. Protooncogene methylation and expression in regenerating liver and preneoplastic liver nodules in the rat by diethylnitrosamine: effect of variations of S-adenosylmethionine:S-adenosylhomocysteine ratio. Carcinogenesis 1989;10:1183–1192. [PubMed: 2472229]
17. Calvisi DF, Ladu S, Gorden A, Farina M, Conner EA, Lee JS, et al. Ubiquitous activation of Ras and Jak/Stat pathways in human HCC. Gastroenterology 2006;130:1117–1128. [PubMed: 16618406]
18. Liu S-P, Li Y-S, Chen Y-J, Chiang E-P, Li AF-Y, Lee Y-H, et al. Glycine N-methyltransferase−/− mice develop chronic hepatitis and glycogen storage disease in the liver. Hepatology 2007;46:1413–1425. [PubMed: 17937387]
19. Yang B, Guo M, Herman JG, Clark DP. Aberrant promoter methylation profiles of tumor suppressor genes in hepatocellular carcinoma. Am J Pathol 2003;163:1101–1107. [PubMed: 12937151]
20. Okochi O, Hibi K, Sakai M, Inoue S, Takeda S, Kaneko T, et al. Methylation-mediated silencing of SOCS-1 gene in hepatocellular carcinoma derived from cirrhosis. Clin Cancer Res 2003;9:5295–5298. [PubMed: 14614012]

21. Eckfeld K, Hesson L, Vos MD, Bieche I, Latif F, Clark GJ. RASSF4/AD037 is a potential ras effector/tumor suppressor of the RASSF family. Cancer Res 2004;64:8688–8693. [PubMed: 15574778]
22. Ogata H, Kobayashi T, Chinen T, Takaki H, Sanada T, Minoda Y, et al. Deletion of the SOCS3 gene in liver parenchymal cells promotes hepatitis-induced hepatocarcinogenesis. Gastroenterology 2006;131:317–319. [PubMed: 16831614]
23. Barski A, Cuddapah S, Cui K, Roh TY, Schones DE, Wang Z, et al. High-resolution profiling of histone methylations in the human genome. Cell 2007;129:823–837. [PubMed: 17512414]
24. Agathanggelou A, Cooper WN, Latuf F. Role of the Ras-association domain family 1 tumor suppressor gene in human cancers. Cancer Res 2005;65:3497–3508. [PubMed: 15867337]
25. Tomasi S, Damman R, Zhang Z, Wang Y, Liu L, Tsark WM, et al. Tumor susceptibility of Rassf1a knockout mice. Cancer Res 2005;65:92–98. [PubMed: 15665283]
26. Esteller M. Cancer epigenomics: DNA methylomes and histone-modification maps. Nat Genet 2007;8:286–298.
27. Lu SC, Alvarez L, Huang ZZ, Chen L, An W, Corrales FJ, et al. Methionine adenosyltransferase 1A knockout mice are predisposed to liver injury and exhibit increased expression of genes involved in proliferation. Proc Natl Acad Sci U S A 2001;98:5560–5565. [PubMed: 11320206]
28. Martínez-Chantar ML, Corrales FJ, Martínez-Cruz A, García-Trevijano ER, Huang ZZ, Chen L, et al. Spontaneous oxidative stress and liver tumors in mice lacking methionine adenosyltransferase 1A. FASEB J 2002;16:1292–1294. [PubMed: 12060674]
29. Robert K, Nehmé J, Bourdon E, Pivert G, Friguet B, Delcayre C, et al. Cystathionine β synthase deficiency promotes oxidative stress, fibrosis, and steatosis in mice liver. Gastroenterology 2005;128:1408–1415.
30. Schwahn BC, Chen Z, Laryea MD, Wendel U, Lussier-Cacan S, Genest J Jr, et al. Homocysteine-betaine interactions in a murine model of 5,10-methylenetetrahydrofolate reductase deficiency. FASEB J 2003;17:512–514. [PubMed: 12551843]

Abbreviations

GNMT
glycine N-methyltransferase

HCC
hepatocellular carcinoma

H3K27me3
trimethylated lysine 27 in histone 3

JAK
Janus kinase

RASSF
Ras-association domain family/tumor suppressor

SAH
S-adenosylhomocysteine

SAMe
S-adenosylmethionine

SOCS
suppressor of cytokine signaling

STAT
signal transducer and activator of transcription

WT

wild type

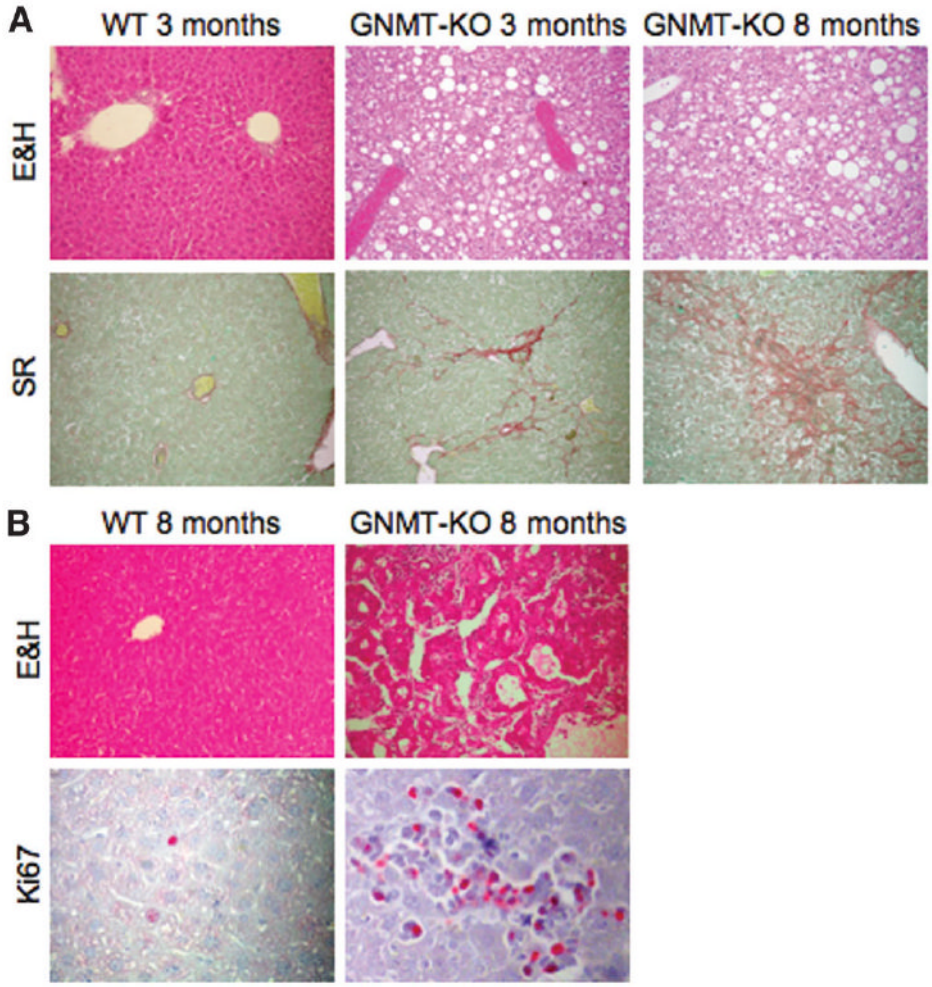

Fig. 1. Deletion of GNMT leads to steatosis, fibrosis, and HCC

(A) At 3 months of age, macro and microvesicular steatosis (white droplets) could be seen through the hepatic lobule in GNMT-knockout (GNMT-KO) mice compared with wild-type (WT) animals. Collagen deposits (stained red) indicate moderate liver fibrosis. By 8 months of age, liver steatosis and fibrosis in mutant mice were more prominent. At least 10 animals per group were examined. (B) At 8 months of age, livers from GNMT-KO mice also had multifocal HCC. Liver cords up to 5 cells thick, lined by endothelial cells, could be seen, with occasional pseudogland formation. Staining with the nuclear proliferation marker Ki67 (red spots) indicates a higher proportion of cells in the cell cycle compared with WT cells. At least 10 animals per group were examined (E&H, eosin and hematoxylin staining; SR, Sirius red staining). Original magnification ×40.

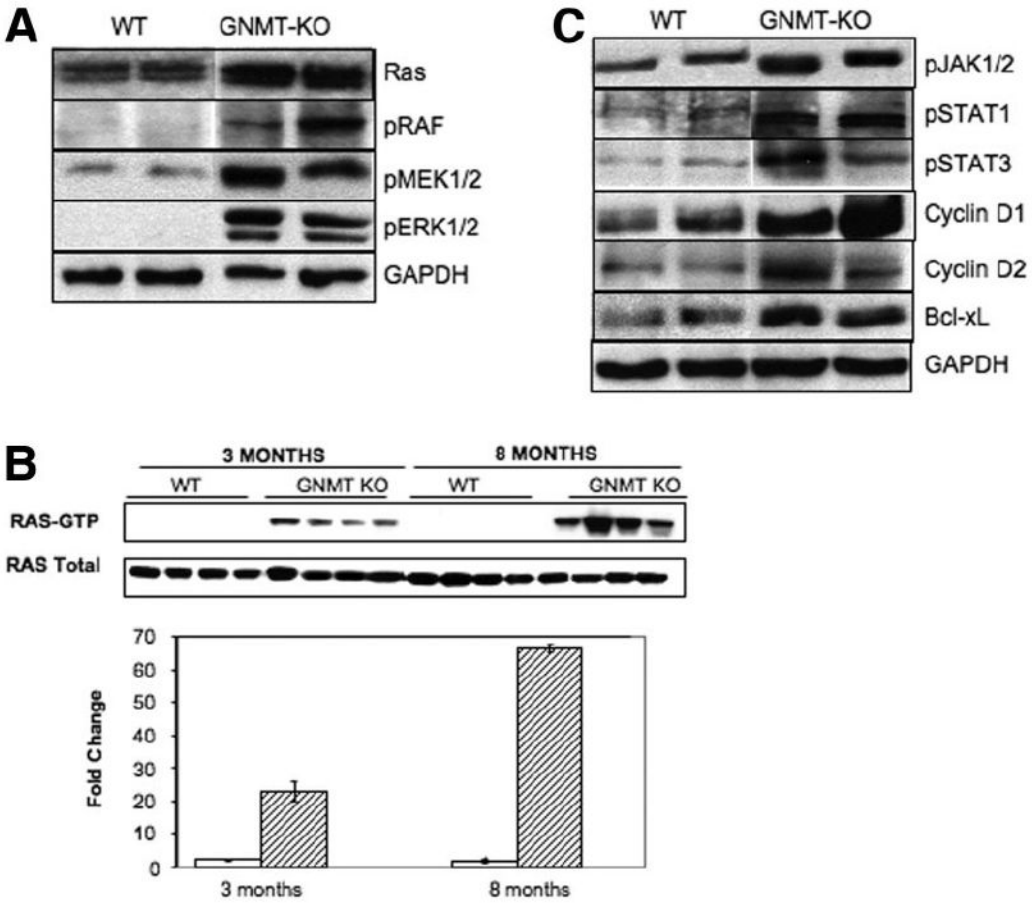

Fig. 2. Activation of Ras and JAK/STAT pathways in GNMT-mutant mice liver

(A) Representative Western blot analysis of Ras downstream effectors (pRAF, pMEK1/2, and pERK1/2). Phosphorylation of RAF, MEK1/2, and ERK1/2 was markedly increased in liver tumors from GNMT-knockout (GNMT-KO) mice as compared with wild-type (WT) animals. One representative data set is shown out of 4 experiments performed. (B) Ras activity, assessed by immunoprecipitation with anti-pan Ras antibody and probed with anti-RAF-1 antibody, was markedly increased in livers from 3-month-old GNMT mice and in liver tumors from 8-month-old GNMT-mutant mice. Four animals from each subgroup were analyzed (WT mice, open bars; GNMT-KO mice, filled bars). (C) Representative Western blot analysis of JAK/STAT downstream effectors (pJAK1/2, pSTAT1, pSTAT3, cyclin D1 and D2, and Bcl-xL). Phosphorylation of JAK1/2, STAT1, and STAT 3 and protein levels of the JAK/STAT target genes, including the proliferation proteins cyclin D1 and cyclin D2 and the antiapoptotic protein Bcl-xL, were markedly increased in liver tumors from GNMT-KO mice. One representative data set is shown of 4 experiments performed. Unless otherwise indicated, animals were all 8 months old.

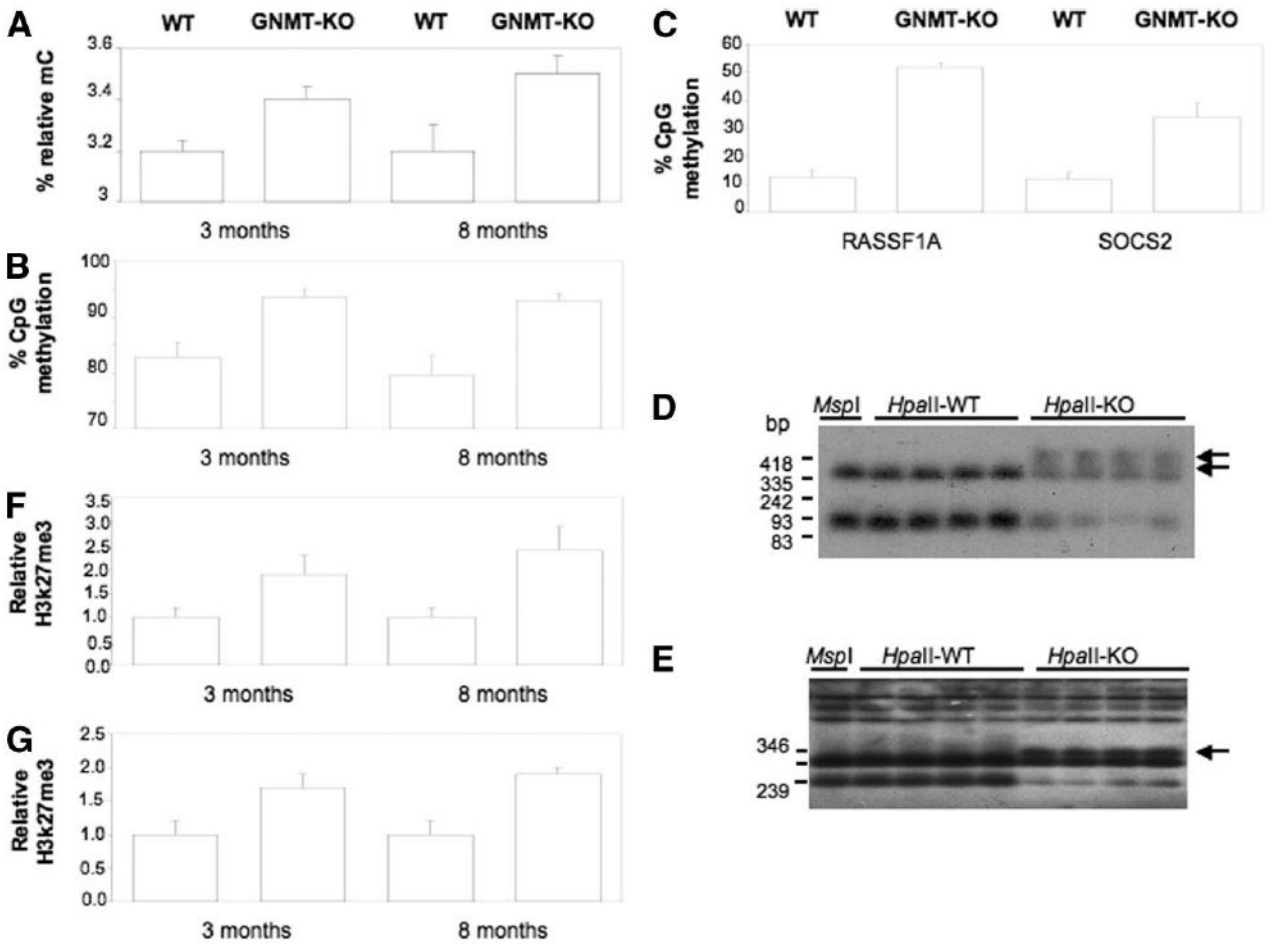

Fig. 3. Deletion of GNMT induces DNA and histone hypermethylation

(A) Quantification of global DNA methylation. Total cytosine and 5-methylcytosine (5mC) content was determined in genomic DNA samples isolated from livers of wild-type (WT) mice at 3 and 8 months of age, in livers from 3-month-old GNMT-knockout (GNMT-KO) mice, and in liver tumors from 8-month-old knockout animals, and relative 5mC content, expressed as the percentage of total cytosine content (methylated and nonmethylated), was determined. Data represent means ± SDs from 5 animals per subgroup (**P* < 0.05 versus WT). (B) Analysis of sequence-specific DNA methylation. CpG DNA methylation of a subtelomeric DNA region at chromosome 1 was determined by PCR analysis after bisulfite modification in samples isolated from livers of 3- and 8-month-old WT mice, in liver samples from 3-month-old GNMT-knockout mice, and in liver tumors from 8-month-old knockout animals. Data represent means ± SDs. from 5 animals per subgroup (**P* < 0.05 versus WT mice). (c–e) Analysis of *RASSF1* and *SOCS2* promoter methylation. (C) To determine the CpG DNA methylation status of *RASSF1* and *SOCS2* promoters in liver samples from 3-month-old mice, we employed bisulfite genomic sequencing because the less sensitive technique, based on the use of *Msp*I and *Hpa*II restriction endonucleases, used at 8 month of age, did not reveal differences between GNMT-knockout and WT livers at 3 month of age. Data represent means ± SDs from 3 animals per subgroup (**P* < 0.05 versus WT). (D, E) To analyze the methylation state of the promoters of *RASSF1* and *SOCS2* at 8 month of age, Southern blot analyses of genomic DNA digested with the methylation-sensitive isoschizomer restriction enzymes *Msp*I and *Hpa*II were performed as described in the Materials and Methods sections. Two *Msp*I fragments were detected in Southern blots when hepatic DNA was hybridized with a

RASSF1 probe (D). All DNA samples from WT mice liver digested with *Hpa*II showed the same pattern of restriction fragments as that produced by *Msp*I digestion, indicating that the CCGG sites were unmethylated. However, all DNA samples from GNMT-KO mice liver tumors digested with *Hpa*II showed additional higher-molecular-weight bands (indicated by an arrow), showing that the *RASSF1* promoter was hypermethylated. When hepatic DNA was hybridized with a SOCS2 probe (E), an additional band (indicated by arrows) was also detected when DNA from GNMT-KO liver tumors was digested with *Hpa*II compared with when digested with *Msp*I, whereas liver samples from WT mice showed the same pattern after digestion with either enzyme (*Hpa*II-WT, DNA samples from WT liver mice digested with *Hpa*II; *Hpa*II-KO, DNA samples from GNMT-KO liver tumors digested with *Hpa*II; 4 animals from each subgroup were analyzed). (F, G) Analysis of H3K27me3 bound to *RASSF1* and *SOCS2*. The amount of H3K27me3 bound to *RASSF1* (F) and *SOCS2* (G) was determined by chromatin immunoprecipitation, as described in the Materials and Methods section in liver samples of 3- and 8-month-old WT mice, in liver samples of 3-month-old GNMT-knockout mice, and in liver tumors from 8-month-old knockout animals. Relative values of H3K27me3 are shown. Data represent means ± SDs from 5 animals per subgroup (*$P < 0.05$ versus WT).

Table 1

Serum Methionine (Met), S-Adenosylmethionine (SAMe), and Aminotransferases (ALT and AST) in 3-Month-Old and 8-Month-Old Wild-Type (WT) and GNMT-Deficient (GNMT-KO) Mice

	WT (3 months)	GNMT-KO (3 months)	WT (8 months)	GNMT-KO (8 months)
Met (μmol/L)	24.9 ± 2.7	81.9 ± 23.3*	51.6 ± 7.5	151 ± 55.0*
SAMe (μmol/L)	0.5 ± 0.05	0.9 ± 0.2*	0.6 ± 0.1	1.2 ± 0.4*
ALT (IU/L)	100 ± 26.6	166 ± 45.3*	105 ± 35.6	320 ± 86.2*
AST (IU/L)	47.5 ± 13.3	99.3 ± 35.8*	76.6 ± 19.4	347 ± 134*

Data are the means ± SDs. of at least 5 animals per group.

* $P < 0.05$ WT versus GNMT-KO.

Table 2

Levels of Ras and JAK/STAT Inhibitors in GNMT-Knockout Mice

Gene	Magnitude of change in GNMT-KO versus WT mice at 3 months	*P* value	Magnitude of change in GNMT-KO versus WT mice at 8 months	*P* value
SOCS 1	−2.1	0.007	−1.6	0.040
SOCS 2	−1.8	0.027	−2.5	0.002
SOCS 3	−2.2	0.021	−4.3	0.001
CIS	−2.2	0.017	−4.1	0.040
RASSF 1	−1.9	0.042	−1.6	0.024
RASSF 4	−1.7	0.0003	−2.4	0.010

Levels of JAK/STAT (SOCS1, SOCS2, SOCS3, CIS) and Ras (RASSF1 and RASSF4) inhibitors were determined by quantitative RT-PCR in the livers of wild-type (WT) mice at 3 and 8 months of age, in liver samples from 3-month-old GNMT-knockout (GNMT-KO) mice, and in liver tumors from 8-month-old knockout mice, normalized using *GAPDH* expression as a housekeeping gene, and the ratio (magnitude of change) of GNMT-KO versus WT calculated. Data represent means of at least 5 animals per subgroup assayed in triplicate.